

# Two Dimensional Classification of the *Swift*/BAT GRBs

E. B. Yang<sup>1</sup> • Z. B. Zhang<sup>1,2,\*</sup> • X. X. Jiang<sup>1</sup>

**Abstract** Using Gaussian Mixture Model and Expectation Maximization algorithm, we have performed a density estimation in the framework of  $T_{90}$  versus hardness ratio for 296 *Swift*/BAT GRBs with known redshift. Here, Bayesian Information Criterion has been taken to compare different models. Our investigations show that two instead of three or more Gaussian components are favoured in both the observer and rest frames. Our key findings are consistent with some previous results.

**Keywords** gamma-ray burst:general– methods: data analysis –methods: statistical

## 1 Introduction

The mystery of Gamma Ray Bursts (GRBs) classification has puzzled astronomers since 1990s. Kouveliotou et al. (1993) firstly discovered the bimodal distribution of  $\log T_{90}$  and proposed the duration classification criterion, that is long GRBs with  $T_{90} > 2s$  and short GRBs with  $T_{90} < 2s$ . This classification method has been widely accepted by many authors so far. The two kinds of GRBs are thought to have different physical origins. Short GRBs are believed to be the product of merging of binary systems, like two neutron stars (NS-NS) or a system of neutron star and black hole (NS-BH) (Nakar 2007; Zhang et al. 2009; Gehrels et al.

2009). LGRBs have close relationship with the collapse of massive stars that has been mostly confirmed by observations (Woosley & Bloom 2006). However, Horváth (1998) analysed the  $\log T_{90}$  distribution of BATSE 3B catalogue including 797 GRBs and found a possible existence of one more class. The phenomenal evidence was also found in the datasets of *BeppoSAX* (Horváth 2009), *Swift*/BAT (Horváth et al. 2008), *Fermi*/GBM (Tarnopolski 2015) etc.

Besides the observed duration distribution, several authors also did similar studies of the distribution in the rest frame. Zhang & Choi (2008) analysed the duration distribution of 95 redshift-known *Swift* GRBs and found that the intrinsic duration is still bimodal. Zitouni et al. (2015) found that 3 groups were statistically better than 2 groups after studying the intrinsic duration distribution of a larger datasets redshift-known *Swift* GRBs, which contains 248 GRBs. Tarnopolski (2016a) analysed the distribution of 947 *Swift* GRBs' observed duration and 347 redshift-known GRBs' duration in both observer and rest frames. It is found that 3 groups are statistically better than 2 groups in the observer frame (see also Tarnopolski 2016b). In the rest frame, 2 groups are good enough for the 347 redshift-known GRBs. Recently, Horváth & Tóth (2016) studied the duration distribution of 888 *Swift* GRBs observed before October 2015. They found that three log-normal function is better to fit the duration distribution than two log-normal function, with a 99.9999% significance level. Their results showed that the relative frequencies were 8%, 35% and 57% for short, intermediate and long bursts, respectively (see also Horváth et al. 2008). They further claimed that no significant differences of the redshift distribution were found between the intermediate GRBs and the long ones. However, the existence of this third class is still controversial so far.

E. B. Yang

Z. B. Zhang

X. X. Jiang

<sup>1</sup>Guizhou University, Department of Physics, College of Sciences, Guiyang 550025, China

<sup>2</sup>Key Laboratory for the Structure and Evolution of Celestial Objects, Chinese Academy of Sciences, Kunming, 650011, China

\* E-mail: sci.zbzhang@gzu.edu.cn

Considering this, durations-based classification of GRBs might not be an only standard. Zhang (2011) proposed that more observational properties, namely *redshift*, *fluence*, *flux*,  $E_{peak}$  of the  $\nu f_\nu$  spectrum and etc., should be taken into account together. Meanwhile, SGRBs usually have harder spectra than LGRBs (Kouveliotou et al. 1993; Zhang & Choi 2008), the clustering phenomenon in the plane of duration versus hardness ratio ( $T_{90}$  vs  $HR$ ) should also be useful to classify the GRBs. Horváth et al. (2006, 2010) did clustering analysis of  $T_{90}$  vs  $HR$  diagram for BATSE and *Swift* datasets, respectively. They found the possible existence of the third class. It is worth noting that the above studies are carried out based on the observations only that may involve the selection effect or bias. In addition, different methods applied for the same sample may reach controversial judgement of GRB classes. To avoid all the above influences, we apply Gaussian Mixture Model (GMM) and Expectation Maximization (EM) Algorithm to the density estimation of  $T_{90}$  vs  $HR$  diagram for the redshift-known *Swift* GRBs in both the observer frame and the rest frame. Note that the sample in this work only comprise of those *Swift*/BAT GRBs with measured redshift, unlike some previous studies. This paper is organized as follows, Section 2 will give the description of our datasets and analysing method. Our main results will be displayed in Section 3.

## 2 Data Preparation and Method

### 2.1 Data Preparation

The current catalog of *Swift*<sup>1</sup> (Donato et al. 2012) contains all GRBs observed by *Swift* from the beginning of the mission, 20 Nov 2004 to 31 Dec 2012, of which 296 bursts have both  $T_{90}$ , redshift, spectral properties (photon index  $\alpha$ , *fluence* and etc.). The observed spectral hardness  $HR_{32,obs}$  in our analysis was defined as the fluence ratio between 50 keV~100 keV and 25 keV~50 keV and it can be calculated by the fluence properties listed in the catalog. To calculate the intrinsic spectral hardness  $HR_{32,int}$ , we use the best fitted spectral model provided in the *Swift* official site. In our datasets, there are 261 GRBs following the single power law model (PL) and other 35 GRBs are better to be described with the cutoff power law model (CPL). The PL and CPL forms can be written as

$$f(E) = \begin{cases} A * E^{-\alpha} \\ A * E^{-\alpha} * e^{-E/\beta} \end{cases} \quad (1)$$

$$(2)$$

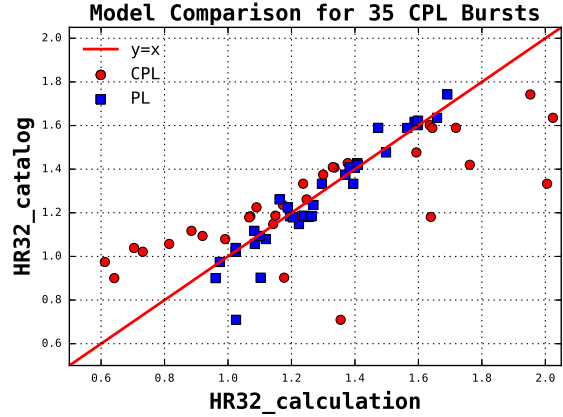


**Fig. 2** Comparing  $HR_{32,obs}$  between the calculated values under PL model and CPL model with the values in catalog for the 35 CPL bursts. Blue squares are calculated by using the PL parameters and red solid points are calculated by using the CPL parameters

where  $\alpha$  are the single power law or the cutoff power law photon index,  $\beta$  is the peak energy, and  $f(E)$  represents the photon flux at a given energy. The hardness ratio can be calculated by

$$HR_{32,obs} = \frac{\int_{50keV}^{100keV} f(E) \cdot E dE}{\int_{25keV}^{50keV} f(E) \cdot E dE} \quad (3)$$

$$HR_{32,int} = \frac{\int_{50*(1+z)keV}^{100*(1+z)keV} f(E') \cdot E' dE'}{\int_{25*(1+z)keV}^{50*(1+z)keV} f(E') \cdot E' dE'} \quad (4)$$

where  $z$  is the cosmological redshift. It is well known in the literature that, with single power law spectrum, the hardness ratio remains the same at any redshift. In the real situation, the hardness ratio should depending on redshift (Bagoly et al. 2003). The spectrum in the rest frame may has got a more complicated form. Considering this, our calculation of hardness ratio in the rest frame, especially for the 261 PL bursts, is simply an approximation of the real value. We also calculate the  $HR_{32,obs}$  by always using the best fitted spectral model and compare it with that in the catalog in Fig. 1. One can find that some points are obviously deviate from the red solid equality line. Considering this, we check the 35 GRBs that follow CPL model and compare the calculated  $HR_{32,obs}$  under both PL model and CPL model with the values in catalog. We compare the two models in Fig. 2, in which the PL form seems more consistent with observations than the CPL one. In order to diagnose if the different model can change the classification based on the  $T_{90}$  distributions, we will do a comparative study with the following method.

<sup>1</sup><http://heasarc.gsfc.nasa.gov/W3Browse/swift/swiftgrb.html>

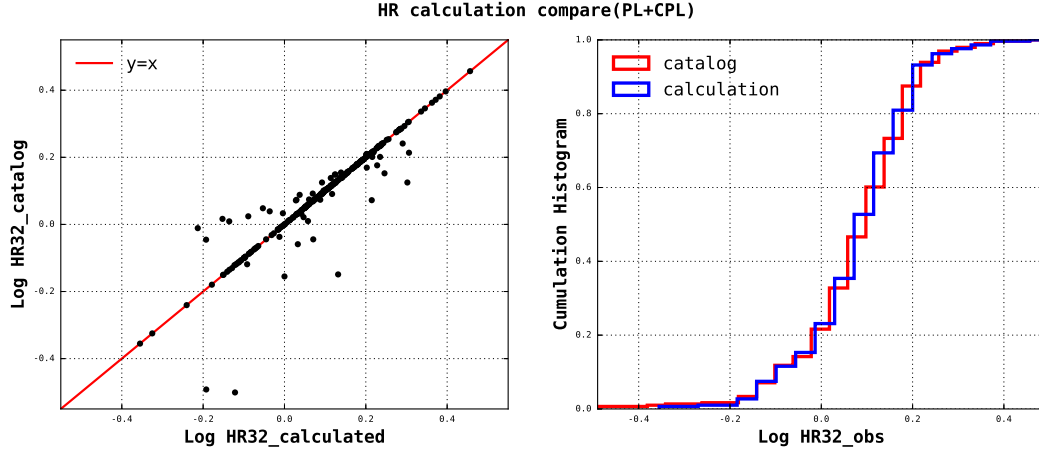


**Fig. 1** Comparing  $HR_{32,obs}$  between our calculation(x axis) and the value(y axis) listed in the catalog on the left panel. The red solid line is the equality line. Their cumulation histograms are compared on the right panel.

## 2.2 Analysis Method

We used the GMM and EM algorithm to estimate the density of *Swift* bursts with known redshift in the  $T_{90} - HR_{32}$  plane. The GMM is a parametric probabilistic function representing a weighted sum of Gaussian components. For the two-dimensional case, the likelihood will be

$$P(\mathbf{X}|\omega, \boldsymbol{\mu}, \boldsymbol{\Sigma}) = \sum_{j=1}^N \left( \sum_{i=1}^k \omega_i N(\mathbf{x}_j | \boldsymbol{\mu}_i, \boldsymbol{\Sigma}_i) \right) \quad (5)$$

where  $\mathbf{X} = \{\mathbf{x}_1, \mathbf{x}_2, \dots, \mathbf{x}_j\}$  is the dataset,  $\omega_i$  is weight of the  $i_{th}$  Gaussian component,  $\boldsymbol{\mu}_i$  and  $\boldsymbol{\Sigma}_i$  are the mean vector and the covariance matrix correspondingly.  $N(\mathbf{x}_j | \boldsymbol{\mu}_i, \boldsymbol{\Sigma}_i)$  is the density of the  $i_{th}$  Gaussian component that can be calculated by

$$N(\mathbf{x}_j | \boldsymbol{\mu}_i, \boldsymbol{\Sigma}_i) = \frac{1}{2\pi} \cdot \frac{1}{\sqrt{|\boldsymbol{\Sigma}_i|}} \cdot \exp \left\{ -\frac{1}{2} (\mathbf{x}_j - \boldsymbol{\mu}_i^T) \boldsymbol{\Sigma}_i^{-1} (\mathbf{x}_j - \boldsymbol{\mu}_i) \right\} \quad (6)$$

The best parameters of an input model can be gained by using the EM algorithm, which will maximize  $\ln P(\mathbf{X}|\omega, \boldsymbol{\mu}, \boldsymbol{\Sigma})$ . In our analysis,  $\boldsymbol{\mu}$  contains two numbers with the order of  $(\log T_{90}, \log HR_{32})$ . The GMM will assign a sample to the Gaussian component with the highest probability.

Bayesian Information Criterion (BIC) (Schwarz 1978; Liddle 2007) were usually used to determine the number of Gaussian components. The BIC value is defined as

$$BIC = p \ln N - 2 \ln P_{max} \quad (7)$$

where  $p$  is the number of parameters,  $P_{max}$  is the maximum likelihood. The BIC will choose the model when Eq. 7 reaches the minimum  $BIC_{min}$ .

$$\Delta = BIC - BIC_{min} \quad (8)$$

For other candidate models, if  $0 < \Delta < 2$ , they are also supported. If  $2 < \Delta < 6$ , they are weakly supported. But if  $\Delta > 6$ , these models are will not be reliable any more (Burnham & Anderson 2004).

All our analyses are performed under *scikit-learn*<sup>2</sup> (Pedregosa et al. 2011), a Python Machine Learning package. The histogram figures were plotted following Knuth bin rule (Knuth 2006) with the implement in *astropy*<sup>3</sup>.

## 3 Results

Using the GMM method, we estimated the  $\log T_{90}$  vs  $\log HR_{32}$  density distribution of 296 redshift-known *Swift* GRBs in both observer and rest frames. Our results are displayed in Fig. 3 and 5 under the mixed spectrum model (marked as “PL+CPL” in the figures), Fig. 4 and 6 under PL only (marked as “PL Only” in the figures). The optimized parameters of different models are listed in Table 1 and Table 2, respectively.

In the observer frame, as shown in Fig. 3, the minimum BIC value obtained with the mixed spectrum model for 2 Gaussian components (2-G) model is  $\sim 223$ , about 6.5 smaller than  $\sim 229$  for 3 Gaussian

<sup>2</sup><http://scikit-learn.org>

<sup>3</sup><http://www.astropy.org>

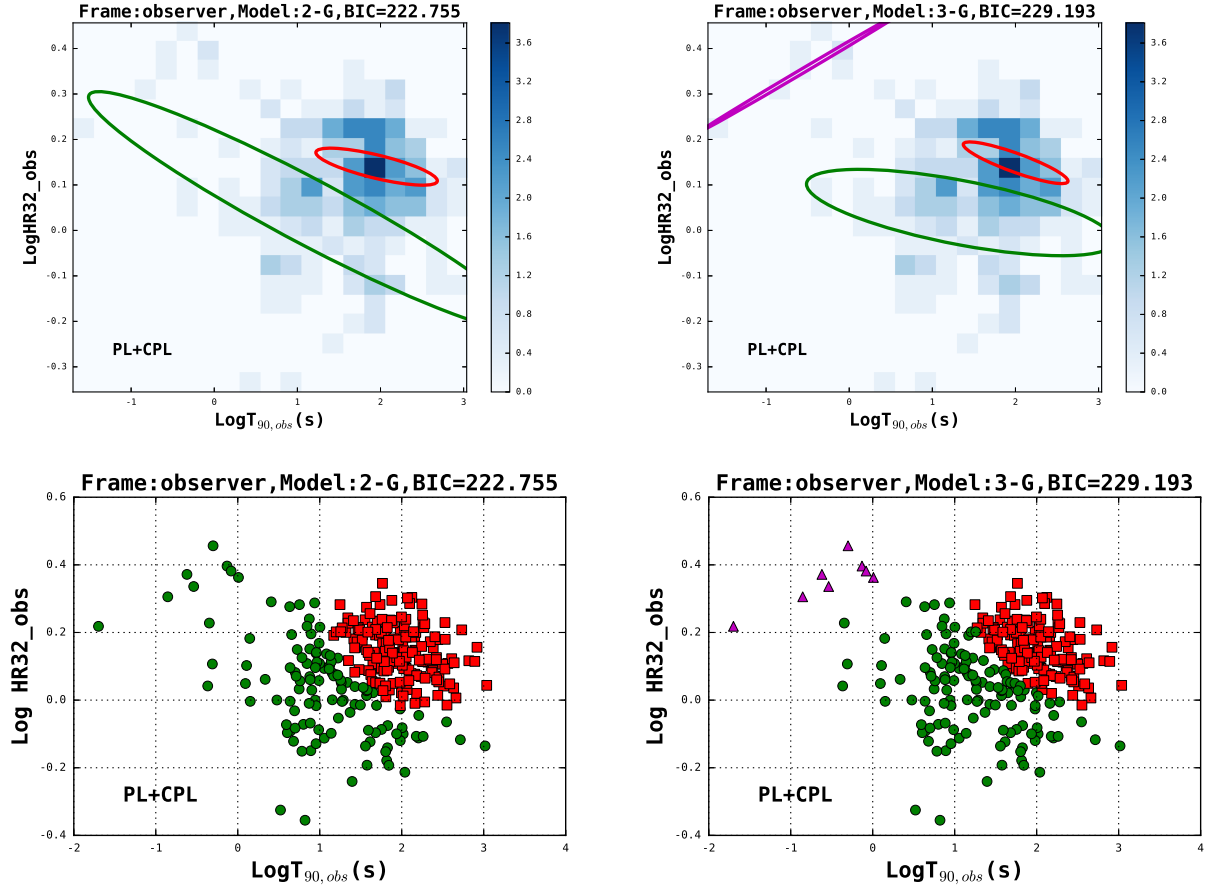


**Fig. 3** GMM analysis results in the observer frame, calculated by mixed spectrum model, PL or CPL. Two figures in the upper panel are the  $1\sigma$  ellipses of the best GMM 2-G model (upper-left) and 3-G model (upper-right), respectively. The background in these two figures are 2 dimensional histogram following Knuth bin rule (Knuth 2006). The lower two figures are the distributions of our datasets. The different symbols with different colors represent those GRBs corresponding to different Gaussian components.

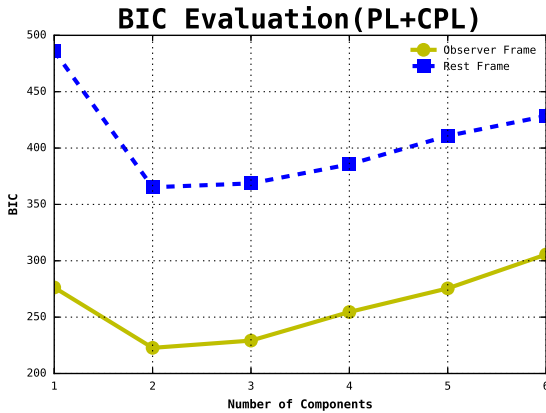


**Fig. 7** BIC evaluation for models with different number of Gaussian components under the calculation by using mixed spectrum model. Yellow solid line is for the observer frame and blue dashed line is for the rest frame.

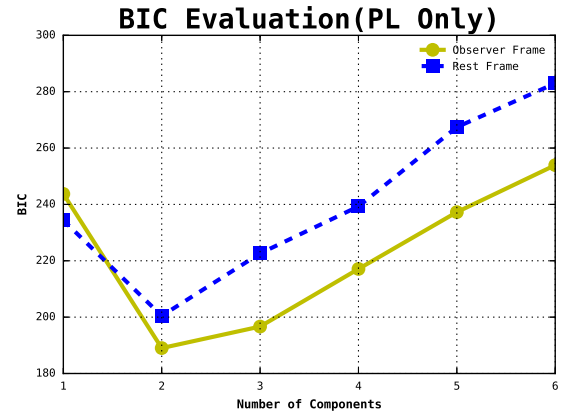


**Fig. 8** Same as Fig. 7, but under the calculation by using the PL only.

components(3-G) model(see Table 1). This indicates

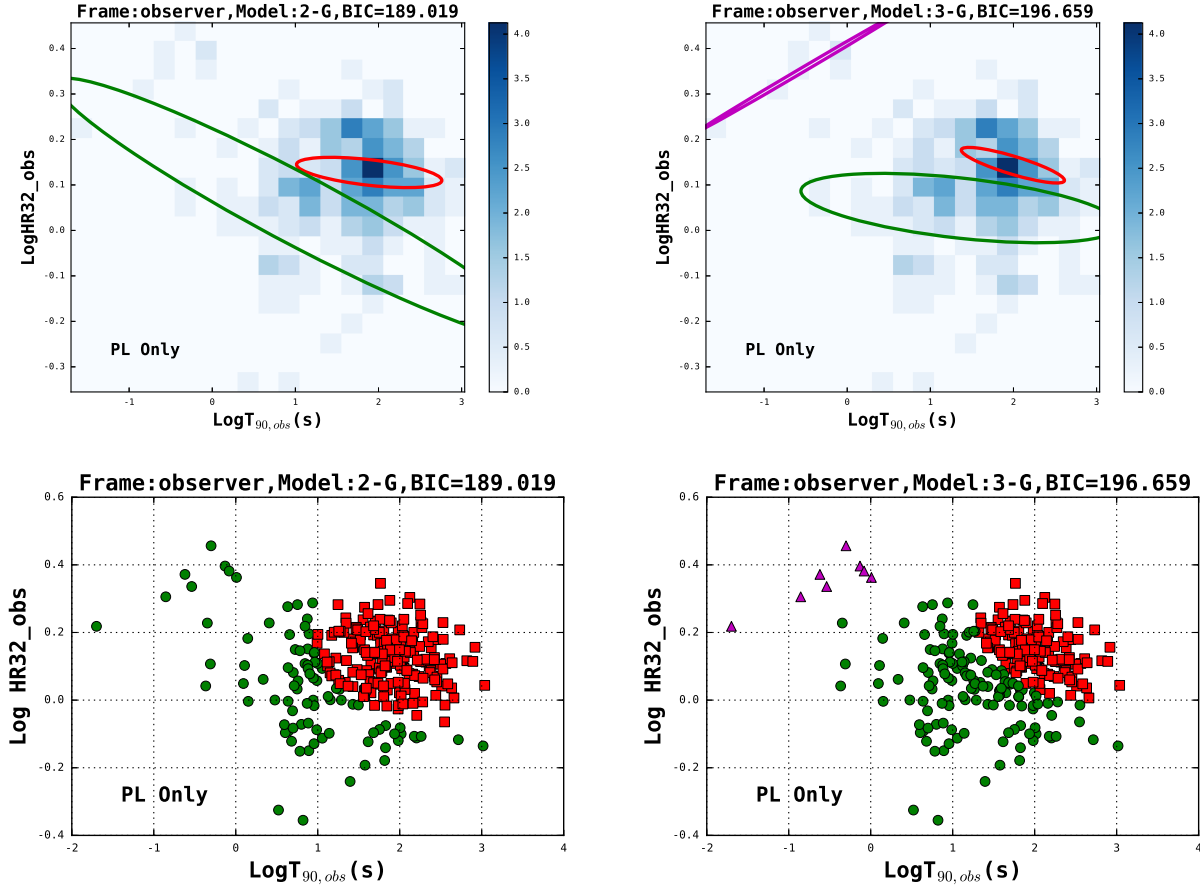


Fig. 4 Same as Fig. 3, but calculated by using PL only.

that 2 components are better enough to describe the two dimensional distribution of  $T_{90,obs} \sim HR_{32,obs}$  in the observer frame. Similar results can also be obtained under the calculation by using PL only in Fig. 4 and Table 2, where minimum BIC value for 2-G is  $\sim 189$ , about 7.7 smaller than  $\sim 197$  for 3-G.

In the rest frame, the intrinsic duration  $T_{90,int}$  can be calculated by  $T_{90,int} = \frac{T_{90,obs}}{(1+z)}$ . The intrinsic  $HR_{32,int}$  is calculated with the Eq. 4. Once again, we find that the BIC prefers the 2-G model instead of the 3-G model. As shown in Fig. 5, and Table 2, by mixture spectral model, the minimum BIC value for 2-G is about 3.4 smaller than 3-G's BIC. For calculation using PL only, the minimum BIC value 3-G is about 22 larger than 2-G's BIC. Simultaneously,  $T_{90,int}$  of the two components move to the smaller value, systematically, as listed in Table 1 and 2.

Fig. 7 and 8 show our BIC evaluation of different models in both observer and rest frames under two calculation condition. One can find that two instead of three or more Gaussian components are favoured in both the observer and rest frames.

Our work shows that 2-G model is better than 3-G model in the observer and rest frames, which is inconsistent with some previous results (e.g. Horváth et al. 2010). For the 3-G model in the observer frame, our analysis returns relative ratios 0.026, 0.508 and 0.466 (PL+CPL) or 0.026, 0.516 and 0.458 (PL only), which are significantly different from 0.079, 0.296 and 0.626 gotten by Horváth et al. (2010) (see also Koen & Bere 2012). Considering the datasets with redshift-known *Swift* GRBs only, the above difference is due to the small fraction of short GRBs in our sample, which makes short GRBs with redshift not statistically significant as a single group possibly. This will be confirmed by a larger population of short GRBs with measured redshift in the future.

Veres et al. (2010) also studied the *Swift*/BAT GRBs and found they favour 3-component model. They argue that the third component is closely related to X-ray Flashes(XRFs). For the mixed spectrum model in Fig. 7, the 3-G model under the calculation by using mixed spectrum model is weakly supported in the rest frame and the third component indeed have the softest spectra (see Fig. 5). This may indicate that the

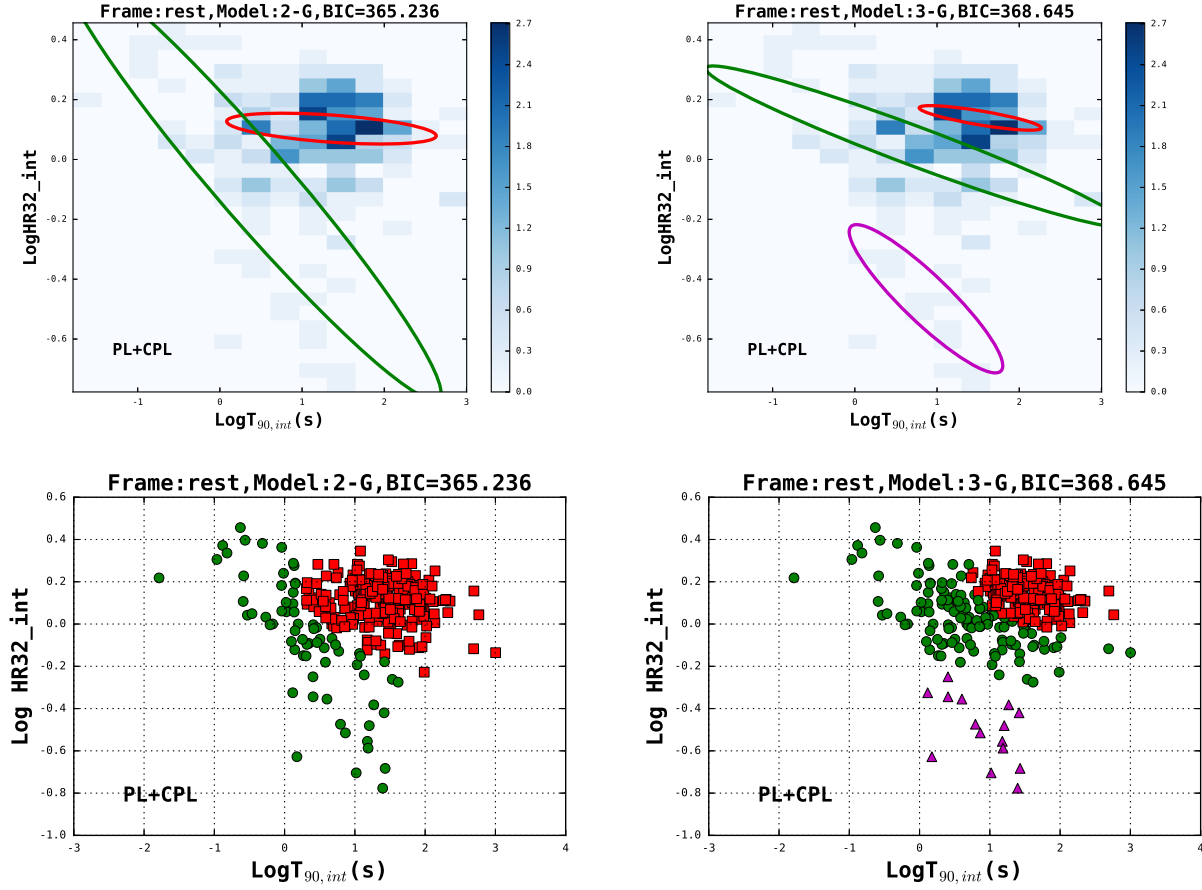


**Fig. 5** GMM analysis results in the rest frame, calculated by using mixed spectrum model, PL or CPL. Order of models are the same as in Fig. 3

connection between the third component and the XRFs might be true. Based on the above analysis in the two dimensional case, one can conclude that the *Swift* bursts with measured redshift are still better to be classified into two groups, which is in good agreement with some previous works (e.g. Zhang & Choi 2008; Qin & Chen 2013; Tarnopolski 2015; Yang et al. 2016)

The results of this work can be summarized as.

1. *Swift* GRBs are better to describe with two groups other than three in either the observer or the rest frame.
2. This classification criterion is not affected by the spectral form too much.
3. The third class weakly supported in the rest frame may correspond to the softest spectra of the XRFs.
4. More redshift-known GRBs are needed to do this kind of research.

**Acknowledgements** We thank the anonymous referee for valuable comments and suggestions that led to an overall improvement of this work. This work

is partly supported by the National Natural Science Foundation of China (Grant No. U1431126; 11263002; 11311140248; 11203026) and Provincial Natural Science Foundations (201519; 20134021; 20117006; OP201511).

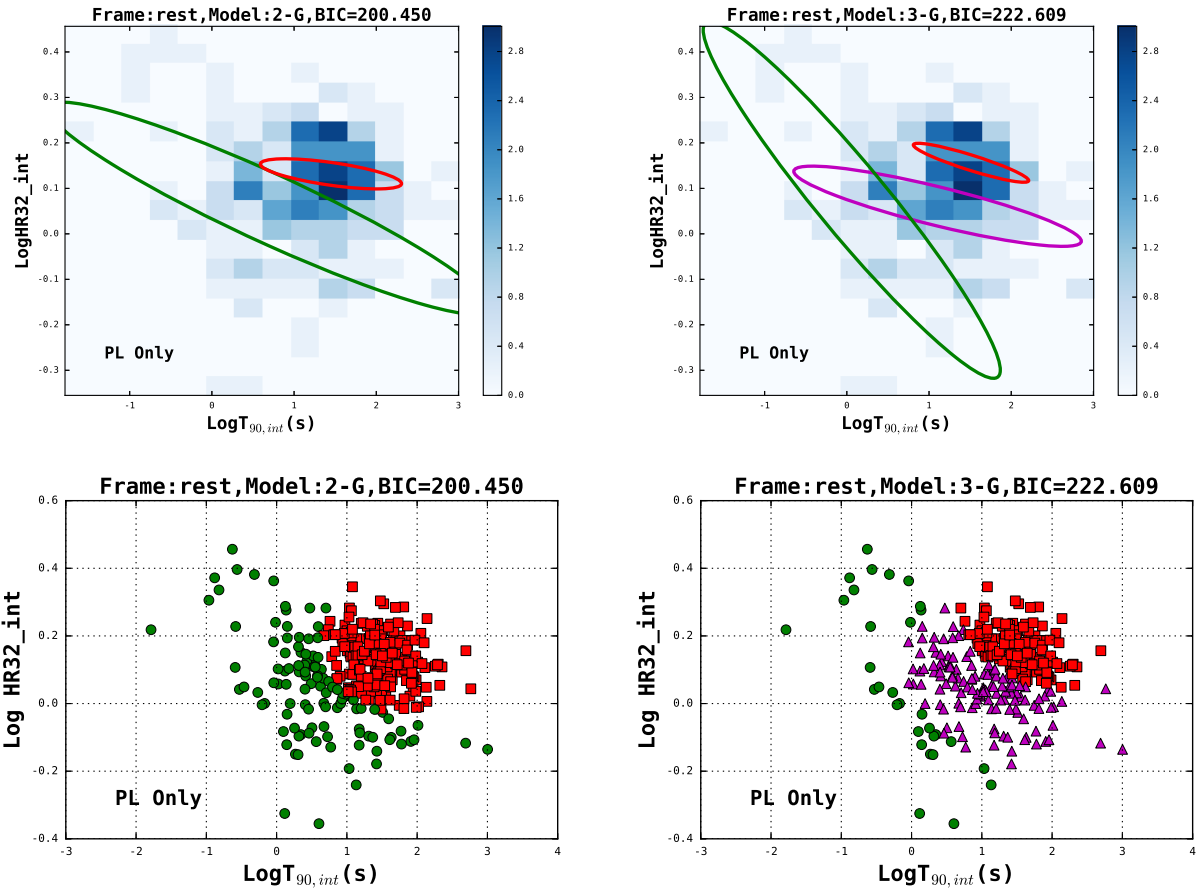


**Fig. 6** Same as Fig. 5, but calculated by using PL only

## References

- Bagoly Z., Csabai I., Mészáros A., et al., 2003, *Astron. Astrophys.*, 398, 919
- Burnham K. P., Anderson D. R., 2004, *Socio. Meth. Res.*, 33, 261
- Donato D., Angelini L., Padgett C. A., et al., 2012, *Astrophys. J. Suppl. Ser.*, 203, 2
- Gehrels N., Ramirez-Ruiz E., Fox D. B., 2009, *Annu. Rev. Astron. Astrophys.*, 47, 567
- Horváth I., 1998, *Astrophys. J.*, 508, 757
- Horváth I., Balázs L. G., Bagoly Z., et al., 2006, *Astron. Astrophys.*, 447, 23
- Horváth I., Balázs L. G., Bagoly Z., et al., 2008, *Astron. Astrophys.*, 489, L1
- Horváth I., 2009, *Astrophys. Space Sci.*, 323, 83
- Horváth I., Bagoly Z., Balázs L. G., et al., 2010, *Astrophys. J.*, 713, 552
- Horváth I., Tóth B. G., 2016, *Astrophys. Space Sci.*, 361, 155
- Koen C, Bere A., 2012, *Mon. Not. R. Astron. Soc.*, 420, 405
- Knuth K. H. 2006, arXiv:0605197
- Kouveliotou C., Meegan C. A., Fishman G. J., et al., 1993, *Astrophys. J.*, 413, L101
- Liddle A. R., 2007, *Mon. Not. R. Astron. Soc.*, 377, L74
- Nakar E., 2007, *Phys. Rep.*, 442, 166

**Table 1** Optimized parameters for redshift-known *Swift* samples in both observer and rest frames. All values are calculated by using mixed spectrum model, PL or CPL.  $\mu$  contains two number with the order of  $(\log T_{90}, \log HR_{32})$ .

PL+CPL						
Frame	$\omega$	$\mu$	$\Sigma$	BIC	$\Delta$	Model
Observer	0.427	(1.121, 0.043)	$\begin{pmatrix} 0.583 & -0.054 \\ -0.054 & 0.023 \end{pmatrix}$	222.755	0	2-G
	0.573	(1.953, 0.140)	$\begin{pmatrix} 0.162 & -0.007 \\ -0.007 & 0.006 \end{pmatrix}$			
	0.026	(-0.542, 0.353)	$\begin{pmatrix} 0.275 & 0.030 \\ 0.030 & 0.004 \end{pmatrix}$	229.193	6.438	3-G
	0.508	(1.337, 0.040)	$\begin{pmatrix} 0.411 & -0.013 \\ -0.013 & 0.016 \end{pmatrix}$			
	0.466	(2.002, 0.149)	$\begin{pmatrix} 0.140 & -0.009 \\ -0.009 & 0.353 \end{pmatrix}$			
	0.229	(0.388, -0.074)	$\begin{pmatrix} 0.492 & -0.139 \\ -0.139 & 0.083 \end{pmatrix}$	365.236	0	2-G
	0.771	(1.357, 0.103)	$\begin{pmatrix} 0.283 & -0.005 \\ -0.005 & 0.010 \end{pmatrix}$			
	0.454	(0.745, 0.043)	$\begin{pmatrix} 0.566 & -0.056 \\ -0.056 & 0.021 \end{pmatrix}$	368.645	3.409	3-G
Rest	0.055	(0.866, -0.465)	$\begin{pmatrix} 0.203 & -0.044 \\ -0.044 & 0.034 \end{pmatrix}$			
	0.491	(1.526, 0.139)	$\begin{pmatrix} 0.165 & -0.007 \\ -0.007 & 0.006 \end{pmatrix}$			

**Table 2** Sample Table. 1, but all values are calculated by using PL only.

PL Only						
Frame	$\omega$	$\mu$	$\Sigma$	BIC	$\Delta$	Model
Observer	0.335	(1.021, 0.045)	$\begin{pmatrix} 0.642 & -0.059 \\ -0.059 & 0.0025 \end{pmatrix}$	189.019	0	2-G
	0.665	(1.887, 0.127)	$\begin{pmatrix} 0.194 & -0.004 \\ -0.004 & 0.006 \end{pmatrix}$			
	0.026	(-0.538, 0.353)	$\begin{pmatrix} 0.273 & 0.029 \\ 0.029 & 0.004 \end{pmatrix}$	196.689	7.670	3-G
	0.516	(1.356, 0.049)	$\begin{pmatrix} 0.424 & -0.008 \\ -0.008 & 0.424 \end{pmatrix}$			
	0.458	(1.993, 0.143)	$\begin{pmatrix} 0.138 & -0.007 \\ -0.007 & 0.005 \end{pmatrix}$			
	0.417	(0.697, 0.056)	$\begin{pmatrix} 0.596 & -0.047 \\ -0.047 & 0.022 \end{pmatrix}$	200.450	0	2-G
	0.583	(1.448, 0.131)	$\begin{pmatrix} 0.191 & -0.005 \\ -0.005 & 0.006 \end{pmatrix}$			
	0.125	(0.060, 0.074)	$\begin{pmatrix} 0.567 & -0.056 \\ -0.056 & 0.021 \end{pmatrix}$	222.609	22.159	3-G
Rest	0.479	(1.104, 0.061)	$\begin{pmatrix} 0.388 & -0.017 \\ -0.017 & 0.020 \end{pmatrix}$			
	0.396	(1.511, 0.156)	$\begin{pmatrix} 0.156 & -0.008 \\ -0.008 & 0.004 \end{pmatrix}$			

- Pedregosa F., Varoquaux G., Gramfort A., et al. , 2011, *The Journal of Machine Learning Research*, 12, 2825
- Qin Y. P., Chen Z. F., 2013, *Mon. Not. R. Astron. Soc.*, 430, 163
- Schwarz G., 1978, *Annals of Statistics*, 6, 461



- 
- Tarnopolski M., 2015, *Astron. Astrophys.*, 581, A29
- Tarnopolski M., 2016a. *New Astron.*, 46, 54
- Tarnopolski M., 2016b. *Mon. Not. R. Astron. Soc.*, 458, 2024
- Veres P., Bagoly Z., Horváth I., et al., 2010, *Astrophys. J.*, 725, 1955
- Woosley S. E., Bloom J. S., 2006, *Annu. Rev. Astron. Astrophys.*, 44, 507
- Yang E. B., Zhang Z. B., Choi C. S., et al., 2016, arxiv: 1603.03680, *Mon. Not. R. Astron. Soc.* submitted
- Zhang B., Zhang B. B., Virgili F. J., et al., 2009, *Astrophys. J.*, 703, 1696
- Zhang B., 2011, *Comptes Rendus Physique*, 12, 206
- Zhang Z. B., Choi C. S., 2008, *Astron. Astrophys.*, 484, 293
- Zitouni H., Guessoum N., Azzam W. J., et al., 2015, *Astrophys. Space Sci.*, 357, 7